

Convective intensification of magnetic flux tubes in stellar photospheres

S. P. Rajaguru¹, R. L. Kurucz² and S. S. Hasan¹

ABSTRACT

The convective collapse of thin magnetic flux tubes in the photospheres of sun-like stars is investigated using realistic models of the superadiabatic upper convection zone layers of these stars. The strengths of convectively stable flux tubes are computed as a function of surface gravity and effective temperature. We find that while stars with $T_{eff} \geq 5500$ K and $\log g \geq 4.0$ show flux tubes highly evacuated of gas, and hence strong field strengths, due to convective collapse, cooler stars exhibit flux tubes with lower field strengths. Observations reveal the existence of field strengths close to thermal equipartition limits even in cooler stars, implying highly evacuated tubes, for which we suggest possible reasons.

Subject headings: stars: atmospheres—stars: magnetic fields—instabilities—MHD

1. Introduction

An important physical quantity basic to the understanding of stellar magnetism is the field strength in small-scale flux tubes and spots on the photospheres. Measurements and interpretation of magnetic field strengths (Saar 1988, 1996a; Guenther 1997) in cool main-sequence stars other than the Sun have been a subject of much debate recently (Basri et al. 1990; Safier 1999), because of the difficulties associated with the modeling of the atmospheric structural changes that the inhomogeneous fibril state of the magnetic field introduces (Basri et al. 1990). However, recent improvements in observing techniques (Saar 1996a; Donati et al. 1997; Johns-Krull et al. 1999) have increased the reliability of observational determination of stellar magnetic field strengths. The observed Zeeman broadening on cool stars is believed to be produced by small flux tubes that appear bright, similar to the solar magnetic network

¹Indian Institute of Astrophysics, Bangalore, India.

²Center for Astrophysics, 60 Garden Street, Cambridge, MA 02138, USA

and facular bright points, rather than spots, which are much fainter than quiet photospheres and hence contribute little to the stellar profiles (Basri et al. 1990; Safer 1999).

Based on measurements of Zeeman effect in cool main sequence stars Saar (1994, 1996a) has inferred that the magnetic field strengths are close to the thermal equipartition field strengths $B_{eq} = \sqrt{8\pi p_e}$ at the observed levels in the atmosphere, where p_e is the gas pressure in the unmagnetised atmosphere, with a conclusion that the surface distribution is in the form of highly evacuated small flux tubes in pressure balance with the ambient atmosphere. Various other measurements (Saar & Linsky 1985; Basri & Marcy 1994; Johns-Krull et al. 1999) also establish such field strengths leading to the general acceptance (Linsky 1999) that stellar surface field strengths scale as the square root of the surface gas pressure. We note that B_{eq} , at any geometrical level in a stellar atmosphere, is the maximum possible field strength for flux tubes confined by gas pressure and can be easily determined (Bunte & Saar 1993; Safer 1999) as a function of $\log g$ and T_{eff} using atmospheric models (e.g., Kurucz (1993)), where g and T_{eff} denote the surface gravity and effective temperature.

The widely accepted mechanism to account for the kG range field strengths in solar magnetic flux tubes is the superadiabatic effect or convective collapse (CC, hereafter) (Parker 1978; Spruit & Zweibel 1979). In this Letter, we report results from a study of this mechanism in the stellar context and test its efficiency as a function of $\log g$ and T_{eff} .

Concentration of magnetic fields into discrete flux tubes or sheaths has long been recognised as a general consequence of the interaction between magnetic fields and cellular convection that expels the flux into downdrafts (Parker 1963; Galloway & Weiss 1981; Proctor & Weiss 1982). High-resolution observations of solar surface magnetic fields confirm the operation of such flux expulsion process. The CC, which is a consequence of thermal insulation of the expelled magnetic flux against convective motions and the superadiabatic thermal stratification of the ambient atmosphere, further intensifies the field to observed values (Parker 1978). It is a convective instability, modified by the magnetic field, and drives a down flow along the field lines of a flux concentration leading to the evacuation of gas inside; lateral pressure balance ensures that a highly compressed intense field flux tube or sheath is formed. This instability develops very rapidly, typically on a free-fall time scale, and is faster than other MHD instabilities present. Hence, the criterion for convective stability can be regarded as a test to check for the occurrence of flux tubes in stars. On the Sun, this instability has a typical growth time of about 2 - 5 minutes (Hasan 1984; Rajaguru & Hasan 2000). Other important instabilities are the interchange instability (Parker 1975; Piddington 1975) connected with the field topology, which has been studied in the stellar context by Bunte & Saar (1993), and the Kelvin- Helmholtz instability (Schussler 1979; Tsinganos 1980) connected with the relative motion between the field confined and the surrounding gas.

We use model atmospheres constructed using the ATLAS9 model atmosphere code (Kurucz 1993), which can extend the Kurucz (1993) atmospheres to cover deeper regions of the convection zone, to study the CC of thin flux tubes embedded in them. The critical field strengths for the tubes to be stable, which indicate the amount of evacuation that stellar flux tubes undergo as a result of the collapse process, are found.

2. Convective Stability of Stellar Thin Flux Tubes

A simple and very effective modeling of the dynamics of thin flux tubes, including the important effects of stratification and compressibility, is provided by the thin flux tube approximation (Roberts & Webb 1978) to the MHD equations. The thin flux tube equations have proved very useful in the study of small-scale solar magnetic elements and have been successful in explaining a variety of observed phenomena (Solanki 1993 and references therein). We solve the same second order differential equation derived by Spruit & Zweibel (1979) based on linear stability analysis of thin tube equations in the adiabatic limit, which is valid for arbitrary background stratifications, employing a grid of stellar model atmospheres. We do not reproduce the equation here, and we refer the reader to Spruit & Zweibel (1979) for details. The stability of a flux tube is controlled by β , which is the ratio of gas to magnetic pressure inside the tube. Weak field (i.e, high β) flux concentrations that are formed at the downdrafts of convective cells are convectively unstable and collapse until their field strengths reach the critical value at which the instability is quenched. Thus the instability is self-limiting and leads to a lower energy stable equilibrium state for flux tubes (Spruit 1979).

2.1. Stellar Model Atmospheres

Models of stellar convective envelopes that extend downward to depths required to study the CC have been specially constructed, extending the Kurucz (1993) models to cover deeper layers using the ATLAS9 model atmosphere code. The convective flux is calculated using mixing length theory. We computed models, with solar metallicity, by extrapolating the shallower models downward one or two points, reconverging, and then repeating the process until a sufficient depth in the atmosphere was obtained. Though the superadiabatic regions below the stellar surfaces are usually thin, a study of the development of convectively driven motions in flux tubes requires a substantial depth extent downward into the convection zone. For the sun, a depth extent of at least 5000 km is needed for the stability limit to be independent of mechanical conditions at the boundary locations (Rajaguru & Hasan 2000). For stars with $\log(g) \geq 4.5$, the ATLAS9 program fails to construct reliable models of sub-

surface regions upto depths that are required in our study. In those situations we attach adiabatic polytropic models that smoothly match with the models from ATLAS9; we note however that, in these cases, the realistic models from ATLAS9 cover the superadiabatic thin regions that drive the convective instability in the flux tubes. The further extension with a polytropic stratification is needed only to avoid breaking artificially the inertia of the convectively driven down flow from the superadiabatic region above at the location where the shallower ATLAS9 model ends. The depth extents, and two important quantities characterizing the surface layers, viz., superadiabaticity $\delta = \nabla - \nabla_{ad}$, where ∇ and ∇_{ad} are the actual and adiabatic temperature gradients respectively, and adiabatic index Γ_1 , are tabulated in Table 1. The grid of models constructed have T_{eff} in the range 4000 – 7000 K (in steps of 500 K) and $\log g$ in the range 2.5 – 5.0 (in steps of 0.5).

2.2. Convective Stability Limits

We have numerically solved the linear eigenvalue problem (equations [6] and [8] of Spruit & Zweibel (1979)), which determines the growth rates and frequencies of the unstable modes and their eigenfunctions, for stellar flux tubes using atmospheric models described in Section 2.1. The convective mode is the fastest growing and is identified from its eigenfunction which has no node between the boundaries, corresponding to a monotonic downflow or upflow throughout the extent of the tube. The critical values β_c that determine stability against these convective modes are found. Assumption of temperature equality between the flux tube and the ambient medium makes β depth independent (Spruit & Zweibel 1979), and we evaluate the critical field strengths from β_c using values of p_e at the height where the continuum Rosseland optical depth $\tau_c=1$. The above is a good approximation close to the photospheres, because the temperature differences between the flux tube and ambient medium are minimal at these heights, as known from solar observations, and also the superadiabatic layers that drive the convective instability are very close to the photosphere (Table 1). The critical field strengths are then given by $B_c(g, T_{eff}) = \sqrt{8\pi p_e / (1 + \beta_c)} = f_{cc}(g, T_{eff}) B_{eq}(g, T_{eff})$. The factor $f_{cc} = 1 / \sqrt{1 + \beta_c}$ represents the efficiency of CC; a value of $f_{cc}=1$, i.e., $\beta_c=0$, corresponds to zero gas pressure, representing a fully evacuated flux tube. The results are summarised in Figure 1. Shown are the critical field strengths $B_c(\tau_c = 1)$ (solid curve) required for convective stability and the maximum possible field strengths $B_{eq}(\tau_c = 1)$ (dashed curve), as a function of $\log g$ for various values of T_{eff} . The variation of B_{eq} with $\log g$ reflects the fact that the photospheric gas pressure, for hydrostatic equilibrium, varies as g . The dependence of B_c on $\log g$ is modulated by the efficiency of CC, i.e., by $f_{cc}(g, T_{eff})$. Changing f_{cc} , i.e., varying efficiency of CC across the $\log g - T_{eff}$ plane, would determine the trends of B_c that differ from B_{eq} in Fig. 1. To see this behaviour clearly, we have also shown the variation of

f_{cc} (dotted curves) with $\log g$ in Fig. 1. Several trends are seen in the figure. The most striking feature is the increasing efficiency of CC for $\log g > 3.5$ as T_{eff} increases; the maximum efficiency occurs at $\log g = 4$ and $T_{eff} = 6500$ K. For $\log g < 3.5$ all stars show inefficient collapse, although δ increases as $\log g$ decreases for a fixed T_{eff} . Since gravity provides the main accelerating force on a displaced fluid element in a convectively unstable stratification, a large reduction in gravity is expected to weaken the convective motions irrespective of variations in δ . This explains the inefficient CC at low values of $\log g$. For $\log g \geq 3.5$, CC shows varying amount of dependencies on T_{eff} ; the general feature is decreasing efficiency of CC with T_{eff} . The largest differences between B_{eq} and B_c are found for the coolest star considered ($T_{eff} = 4000$ K). For example, for $T_{eff} = 4000$ K and $\log g = 4.5$, B_{eq} and B_c differ by about 1000 G. This inefficient behaviour of CC finds an explanation in Figure 2, where we plot the maximum values of the superadiabaticity δ against T_{eff} for different values of $\log g$; δ decreases monotonically with T_{eff} , for fixed $\log g$, thus explaining the low efficiency of CC in cooler stars. As a general result, we find that CC is not efficient enough in stars cooler than $T_{eff} = 5500$ K, i.e., on the cooler side of the Sun in the main-sequence, owing to the absence of significantly superadiabatic sub-surface thermal structure, to produce field strengths close to B_{eq} .

We emphasise that the stability limits found in this study are from a global analysis and with effects of vertical gradients in ionization and adiabatic index taken into account. There are no known analytic criteria that capture the above effects. An analytic criterion derived by Roberts & Webb (1978) for finite extent vertical thin flux tubes is both necessary and sufficient but for linear (polytropic) temperature profiles and do not include effects of gradients in ionization and adiabatic index. Despite its limitations we use it to compare and understand qualitatively our results. This criterion yields critical values of β given by,

$$\beta_{c,RW} = \frac{\nabla^2}{2\delta} \left[\left(\frac{2\pi}{\ln(H_b/H_0)} \right)^2 + \left(1 - \frac{1}{2\nabla} \right)^2 \right] - 1, \quad (1)$$

where H_b and H_0 are the pressure scale-heights at the bottom and top ends of the flux tube. We have compared values of β_c and $\beta_{c,RW}$ in Table 2, adopting appropriate values for the quantities in Equation 1 from the stellar models used here (since ∇ , and hence δ , is assumed constant in the derivation of Equation 1, a nominal value of 2000 km is used as a representative extent of the flux tube). Though the exact values of β_c and $\beta_{c,RW}$ do not match, owing to the reasons given above, they show similar trends against T_{eff} . It is evident that the weaker field strengths (i.e., larger $\beta_{c,SI}$) for stability in cooler stars is mainly a reflection of smaller δ . Additionally, since the constant temperature gradient of a polytrope is proportional to g , the scale-height ratio in Equation 1 yields small values (≈ 1) at lower values of $\log g$ and hence large values of β_c . We attribute the differences between

the present results and those from Equation 1 to the neglect of gradients in ∇ , ionization and adiabatic index in the derivation of Equation 1. It is noted that since magnetic pressure varies as B^2 and the gas pressure is proportional to g , difference between B_c and B_{eq} would be larger in higher gravity stars for a constant value of β_c .

3. Discussions and Conclusions

We have examined the superadiabatic effect (or CC) (Parker 1978) in the stellar context, using realistic models of the outer convective layers of stars. Our results show that whereas it is possible to produce highly evacuated stable tubes in stars with $T_{eff} \geq 5500$ K through the CC mechanism, it is not so in cooler stars; the decreasing amount of superadiabaticity in the upper convection zone layers of K and M spectral type stars make the CC inefficient yielding field strengths much less than B_{eq} . Hence, if CC is the main physical process responsible for the formation of fibril-like evacuated flux tubes then it is expected that the differences between the observed B and B_{eq} increase as T_{eff} decreases. The existing observational results are not entirely consistent with such a trend as there are several cases of K and M dwarfs having B values close to or even exceeding B_{eq} ; but, all these stars with high B have high filling factors, f , typically 0.5 or higher, which correlate strongly with stellar angular rotation frequency Ω . Rotation-activity correlation dominated through high f values is a well observed fact (Saar 1990, 1996a) consistent with dynamo theory predictions. A careful look at the observational results compiled by Saar (1990) and Solanki (1992) reveal that all the cases of $B < B_{eq}$ also belong to K and M spectral types, but which have smaller Ω and are less active; and all the G type stars show B values tightly around B_{eq} . As an example, from the compilation by Saar (1990), we find that the stars GL 171.2A (BY Dra) and HD 201091, which are of similar spectral type (K5V, $T_{eff} \approx 4400$ K), have widely differing field strengths: 2.8 kG (Saar et al. 1987) and 1.2 kG (Marcy & Basri 1989) respectively. But these field strengths have good correlation with the Ω and f values (rotation periods of 1.85 and 37.9 days and f values of 0.5 and 0.24, respectively). From our results shown in Figure 1, we find for $T_{eff} \approx 4400$ K and a $\log g \approx 4.5$ (main-sequence) a field strength of ≈ 1.3 kG that CC yields, in close agreement with the slow rotating, low f value case of HD 201091. Marcy & Basri (1989) themselves caution that the separation of B and f values is uncertain and that the flux fB is larger than expected for HD 201091. But, their speculation that B remains at the inferred value while f changes by 2 orders of magnitude, which is not inconsistent with the observed time variation in the chromospheric emission, finds support from the present result. The best support for the present calculations comes from a multi-line infra-red Zeeman analysis of ϵ Eridani, a K2 V star with $T_{eff} = 5130$ K and $\log g = 4.7$, by Valenti et al. (1995), who find $f = 0.088$ and $B = 1.44$ kG in close agreement with the value

$B_c \approx 1.4$ kG from Figure 1. It would thus seem that the CC indeed operates on all solar-like main sequence stars producing convectively stable tubes as dictated by the sub-surface superadiabatic structure; and, the higher than expected B values in K and M dwarfs may originate from effects induced by high values of Ω . Recent detections of increased photometric variability in highly active K dwarfs, which exhibit *saturation* in their magnetic activity (O’Dell et al. 1995), indicate that stars with angular velocities $\Omega > \Omega_{sat}$ show increased number of spots. Thus, the present result that $B_c \ll B_{eq}$ for non-spot small scale magnetic fields in stars with $T_{eff} \leq 5000$ K and its agreement with B observed on slow rotators provide a theoretical reason to believe the idea that Ω_{sat} marks a change in contributions from f and B to fB (Saar 1996b): f saturates around 0.6 and $\Omega (> \Omega_{sat})$ begins to contribute to B by increasing f_{spot}/f to maintain the continued increase of flux fB well described by the power-law fits $fB \propto \Omega^{1.3}$ or $fB \propto (\tau_c \Omega)^{1.2}$ to the observations (Saar 1990), where τ_c is the convective turn-over time and $\tau_c \Omega$ is the inverse Rossby number. We suggest that the calculated stability limits B_c can be used to separate f from the observed fluxes fB for slow rotators ($\Omega < \Omega_{sat}$), when there remain otherwise unknown uncertainties in the separation of f and B in observational analyses. The calculations here extend down only to $T_{eff}=4000$ K due to limitations in generating reliable convection zone models for cooler stars, but, by extrapolation, it is likely that CC remains ineffective yielding $B_c(\tau_c = 1) \ll B_{eq}(\tau_c = 1)$ in cooler M dwarfs too. Two similar spectral type M dwarfs, observed by Johns-Krull & Valenti (1996), do show widely differing field strengths, in correlation with their Ω , but the lower Ω star seems to show B larger than the likely B_c . Future refinements, both in observations and theory, are needed to understand fields in M dwarfs.

We note that the thin tube approximation does not get constrained by increasing f ; as long as the distribution of flux remains in the form of small flux tubes dominating the observed spectral profiles, the present results on B_c can be used in the interpretation of observations. Thus, if the observed profiles do arise only from non-spot fields even in fast rotating K and M dwarfs which show $B \gg B_c$ then the present results call for new physical mechanisms to produce highly evacuated tubes, which are likely not due to thermodynamic reasons but due to fast-rotation induced phenomena. This may imply a failure of solar analogy as far as the formation and dynamics of surface magnetic fields are concerned. We conclude by pointing out that, in any case, the convective stability limits calculated here need to be satisfied by pressure confined flux tubes and thus may serve as useful lower limits.

We are thankful to an anonymous referee for constructive comments.

REFERENCES

- Basri, G., Marcy, G. W., & Valenti, J. A. 1990, *ApJ*, 360, 650
- Basri, G., & Marcy, G. W. 1994, *ApJ*, 431, 844
- Bunte, M., & Saar, S. H. 1993, *A&A*, 271, 167
- Donati, J.-F., Semel, M., Carter, B. D., Rees, D. E., & Collier Cameron, A. 1997, *MNRAS*, 291, 658
- Galloway, D. J., & Weiss, N. O. 1981, *ApJ*, 243, 945
- Guenther, E. W. 1997, in *Herbig-Haro Flows and the Birth of Low-mass Stars*, ed. B. Reipurth & C. Bertout (Dordrecht: Kluwer), 465
- Hasan, S. S. 1984, *ApJ*, 285, 851
- Johns-Krull, C. M., & Valenti, J. A. 1996, *ApJ*, 459, L95
- Johns-Krull, C. M., Valenti, J. A., Hatzes, A. P., & Kanaan, A. 1999, *ApJ*, 510, L39
- Kurucz, R. L. 1993, *ATLAS9 Stellar Atmosphere Programs and 2 km/s grid*, Kurucz CD-ROM No.13. Cambridge, Mass.: Smithsonian Astrophysical Observatory.
- Linsky, J. 1999, in *Solar and Stellar Activity: Similarities and Differences*, ASP Conference Series 158, eds. C. J. Butler and J. G. Doyle, p3
- Marcy, G. W., & Basri, G. 1989, *ApJ*, 345, 480
- O'Dell, M. A., Panagi, P., Hendry, M. A., & Collier Cameron, A. 1995, *A&A*, 294, 715
- Parker, E. N. 1963, *ApJ*, 138, 552
- Parker, E. N. 1975, *Sol. Phys.*, 40, 291
- Parker, E. N. 1978, *ApJ*, 221, 368
- Piddington, J. H. 1975, *Ap&SS*, 34, 347
- Proctor, M. R. E., Weiss, N. O. 1982, *Rep. Progr. Phys.*, 45, 1317
- Rajaguru, S. P. & Hasan, S. S. 2000, *ApJ*, 544, 522
- Roberts, B. & Webb, A. R. 1978, *Sol. Phys.*, 56, 5

- Saar, S. H. 1988, ApJ, 324, 441
- Saar, S. H. 1990, in IAU Symposium No. 138 Solar Photosphere: Structure, Convection, and Magnetic Fields, ed. J. O. Stenflo (Kluwer: Dordrecht), p427
- Saar, S. H. 1994, in IAU Symposium No. 154, ed. D. M. Rabin, John T. Jefferies, C. Lindsey (Kluwer: Dordrecht), p493 and p437
- Saar, S. H. 1996, in IAU Symposium No. 176, ed. Klaus G. Strassmeier, Jeffrey L. Linsky (Kluwer: Dordrecht), p237
- Saar, S. H. 1996, in IAU Colloquium 153 on Magnetodynamic Phenomena in the Solar Atmosphere - Prototypes of of Stellar Magnetic Activity, ed. Y. Uchida, T. Kosugi, & H. S. Hudson (Kluwer Academic Publishers), p367
- Saar, S. H., Linsky, J. L., & Giampapa, M. S. 1987, in 27th Liege International Astrophysical Colloquium: Observational Astrophysics With High Precision Data, eds. L. Delbouille and A. Monfils, Universite de Liege, Liege, p. 103
- Saar, S. H. & Linsky, J. 1985, ApJ, 299, L47
- Safier, P. N. 1999, ApJ, 510, L127
- Schussler, M. 1979, A&A, 71, 79
- Solanki, S. K. 1992, in Seventh Cambridge Workshop on Cool Stars, Stellar Systems, and the Sun, ed. M. S. Giampapa & J. A. Bookbinder, ASP Conf. Series, Vol. 26, 211
- Spruit, H. C. 1979, Sol. Phys., 61, 363
- Spruit, H. C. & Zweibel, E. G. 1979, Sol. Phys., 62, 15
- Tsinganos, K. C. 1980, ApJ, 239, 746
- Valenti, J. A., Marcy, G. W., & Basri, G. 1995, ApJ, 439, 939

Table 1: Characteristics of Model Atmospheres

T_{eff} (K)	$\log g$								
	4.0			4.5			5		
	Depth (km.)	δ_{max} ($z=$ km)	Γ_1 (at δ_{max})	Depth (km)	δ_{max} ($z=$ km)	Γ_1 (at δ_{max})	Depth (km)	δ_{max} ($z=$ km)	Γ_1 (at δ_{max})
4000	3610	0.2306 ($z=60$ km)	1.665	1270	0.3173 ($z=30$ km)	1.663	295	0.0525 ($z=60$ km)	1.636
4500	4693	0.4606 ($z=230$ km)	1.590	1206	0.2596 ($z=80$ km)	1.593	423	0.1422 ($z=30$ km)	1.592
5000	5573	0.9000 ($z=180$ km)	1.553	1382	0.4735 ($z=70$ km)	1.544	435	0.2450 ($z=30$ km)	1.515
5500	8300	1.2635 ($z=130$ km)	1.296	1604	0.7310 ($z=50$ km)	1.466	606	0.5004 ($z=20$ km)	1.446
6000	9030	1.627 ($z=80$ km)	1.369	2012	1.041 ($z=30$ km)	1.415	720	0.6028 ($z=10$ km)	1.501
6500	108487	1.936 ($z=60$ km)	1.277	3472	1.318 ($z=20$ km)	1.341	960	0.8546 ($z=10$ km)	1.265

Table 2: Comparison of Critical Values of β

T_{eff}	$\log g$					
	4.0		4.5		5	
	β_c	$\beta_{c,RW}$	β_c	$\beta_{c,RW}$	β_c	$\beta_{c,RW}$
4000	1.81	7.76	2.06	2.57	14.44	6.90
4500	1.19	7.32	1.98	3.37	3.94	2.16
5000	0.74	6.20	1.13	2.54	2.56	1.20
5500	0.38	6.17	0.52	2.35	1.18	0.78
6000	0.27	6.44	0.19	2.44	0.54	0.86
6500	0.12	6.95	0.1	2.58	0.16	0.76

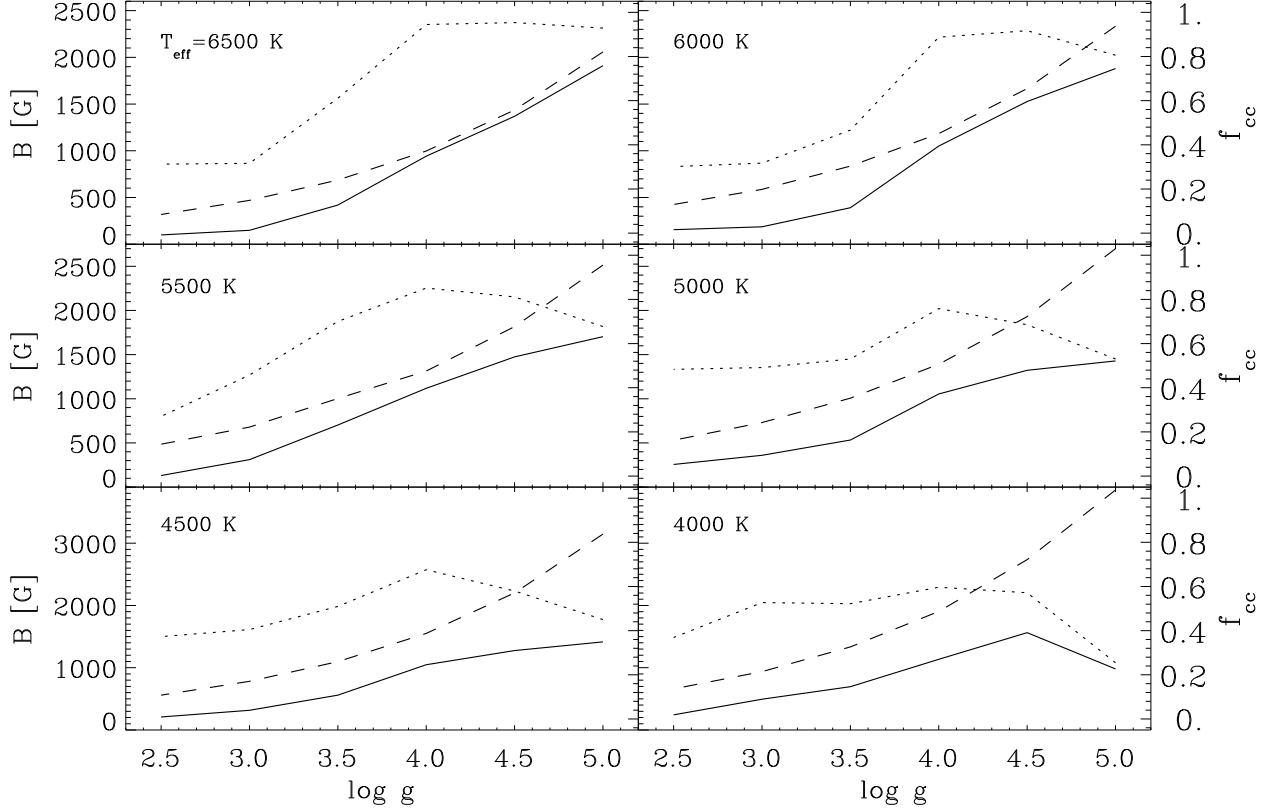


Fig. 1.— The critical magnetic field strengths $B_c(\tau_c = 1)$ for convective stability (*solid lines*) and thermal equipartition limits $B_{eq}(\tau_c = 1)$ (*dashed lines*), against $\log g$ for various T_{eff} . B_c correspond to those that can be achieved by convective collapse and B_{eq} are the maximum possible field strengths for flux tubes. Efficiencies of CC, f_{cc} , are shown as *dotted* curves and correspond to right-side ordinates of the panels.

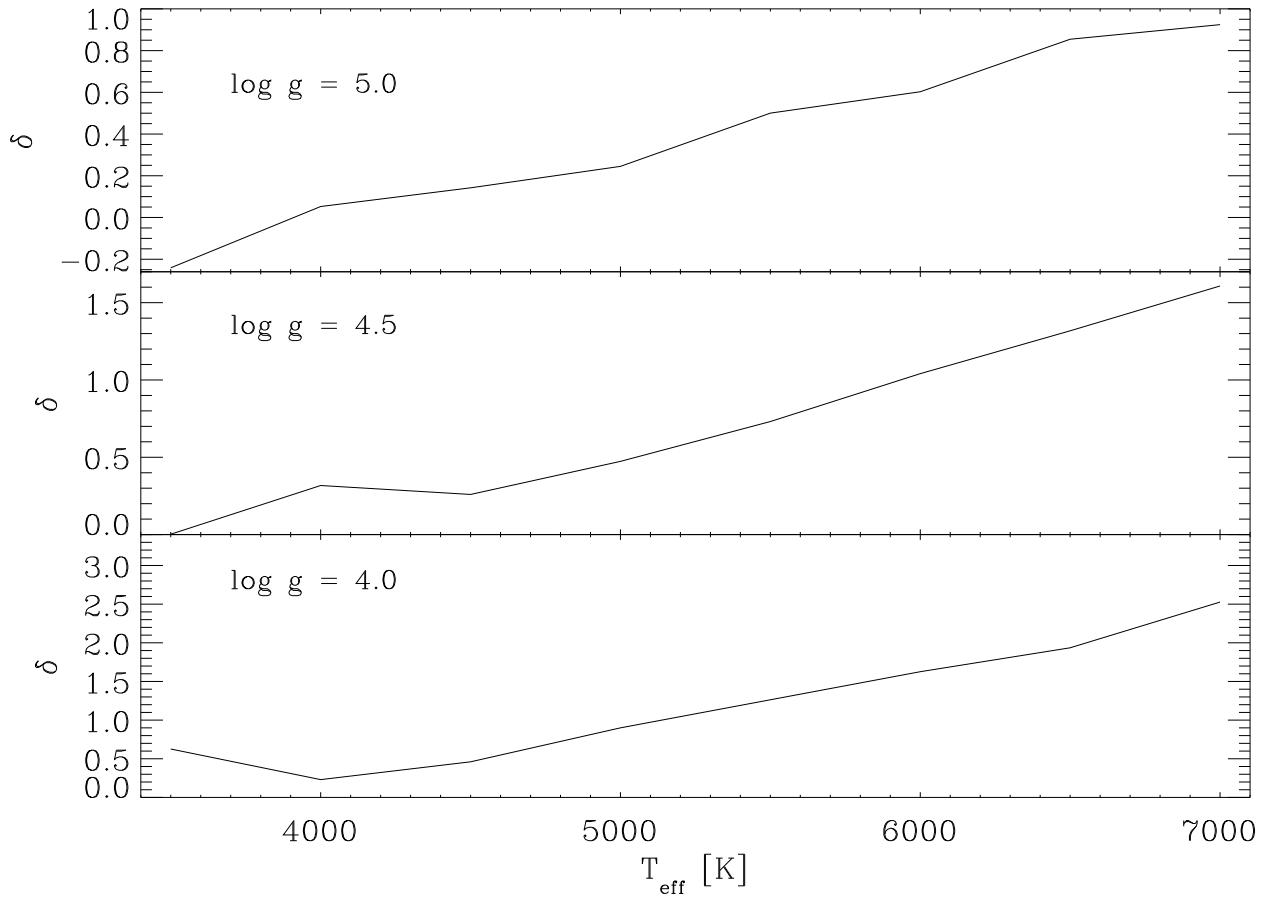


Fig. 2.— The peak values of superadiabaticity $\delta = \nabla - \nabla_a$ that characterize the sub-surface upper convective layers as a function of T_{eff} for three different values of $\log g$.